Synthesis and Characterization of Dirhodium(II,II)−Porphyrin-Based Multiredox Systems

Sandra Lo Schiavo,*[a] Scolastica Serroni,[a] Fausto Puntoriero,[a] Giuseppe Tresoldi,[a] and Pasquale Piraino[a]

Keywords: Rhodium / Porphyrins / Electrochemistry / Luminescence

Dirhodium(II,II)–porphyrin-based multiredox systems were easily prepared by combining the versatile reactivity, both axial and equatorial, of the $[Rh_2(form)_2(O_2CCF_3)_2(H_2O)_2]$ (form = *N*,*N*′-di-*p*-tolylformamidinate) complex and the well-known coordination capability of *meso*-substituted phenylporphyrins. In this way, redox systems featured by porphyrins axially or equatorially coordinated to the dirhodium subunits were obtained. Electrochemical and luminescence properties of the new assemblies were also investigated. Porphyrin–dirhodium(II,II) multiredox assemblies were synthesized by exploiting both the classical axial and the peculiar equatorial reactivity of the complex $[Rh_2(form)_2(O_2CCF_3)_2(H_2O)_2]$ (**1**) (form = *N*,*N*′-di-*p*-tolylformamidinate). The species $[Rh_2(form)_2(PCOO)_2]$ (**2**), featuring two bridged (carboxyphenyl)porphyrins in the equatorial positions, was prepared by metathetical reaction of **1** with the sodium salt of *meso*-5-(4-carboxyphenyl)-5,10,15-triphenylporphyrin (PCOO). Conversely, redox systems in which porphyrins are axially ligated to dirhodium were obtained by treating **1** with a variety of functionalized *meso*-pyridylporphyrins. Depending on the number and position of the peripheral pyridyl substituents, assemblies with different nuclearity, both in terms of metal and porphyrin subunits, were isolated. The 1:2 dirhodium/porphyrin adduct, $[Rh_2(form)_2(O_2CCF_3)_2(PyP)_2]$ (**3**) was obtained by treatment of **1** with triphenyl(pyridyl)porphyrin (PyP). By combination of **1** with the *cis*-5,10-diphenyl-15,20-dipyridylporphyrin (*cis*-DPyP) the molecular square box, $[Rh_2(form)_2(CF_3CO_2)_2(cis\text{-DPyP})]_4$ (**4**) was isolated in good yield. The reaction of **1** with 5,10,15,20-tetrakis(4-pyridyl)porphyrin (TPyP) is dependent on the experimental conditions and led to two different products: the grid polymer $[\{Rh_2(form)_2(CF_3CO_2)_2\}_2(TPyP)]_n$ (**5**) and the symmetric tetramer $[\{Rh_2(form)_2(CF_3CO_2)_2\}_4(TPyP)]$ (**6**), respectively. All the products were characterized by conventional spectroscopic methods. Proton NMR spectroscopy resulted particularly useful for the characterization of dirhodium–phenyl(pyridyl)porphyrin aggregates. The 2,6-pyridyl proton resonances are highly affected by coordination and experience significantly upfield shifts with respect to the corresponding unbound porphyrin. Systems **2**, **3**, **4**, and **6** underwent many redox processes in the potential window under investigation (+2; −1.4 V), each one of them can be assigned to the specific subunits of the molecular arrays. The emission studies performed on the same aggregates revealed that the porphyrin-based emission was significantly quenched by, most likely, reductive electron transfer from dirhodium subunits to the excited porphyrin chromophores. Such a process appears to be larger in the pyridylporphyrin–dirhodium systems with respect to the (carboxyphenyl)porphyrin ones.

Introduction

Redox multicomponent systems continue to be a topic of current interest owing to their diverse potential of application in the field of the molecular materials. Apart from their molecular properties (magnetism, electrical conductivity) these systems, depending on their structural features, may also display interesting specific functions (catalytic, host−guest interactions, electron reservoir, etc.) or act as models for electron or energy transport.[1] The choice of the redox components represents a crucial point in the synthetic approach to redox systems. The inclusion of transition metals constitutes one of the most promising means of introducing redox activity in a multicomponent system. These, besides acting as redox-active moieties, may play an important role from a synthetic point of view.[2] In fact, the self-assembly by metal complexation has provided a widely used route to supramolecular arrays.

Our experience in the chemistry of redox-active dirhodium(II,II) complexes, with lantern structures, led us to explore the possibility to build dirhodium multiredox based systems. By exploiting the metal-mediated self-assembly process, we recently succeeded in preparing a series of multiredox molecular square boxes incorporating two or four dirhodium(II,II) units, as redox metal centres, and dicarboxylate dianions as connectors.[3] The electrochemical

[a] Dipartimento di Chimica Inorganica, Chimica Analitica e Chimica Fisica, Università di Messina,
Salita Sperone n. 31, 98166 Vil. S. Agata, Messina, Italy
E-mail: loschiavo@chem.unime.it

  1434−1948/02/0101−0079 $ 17.50+.50/0

investigations performed on these square boxes $[Rh_2(form)_2(dicarboxylate)]_4$ [form = *N*,*N*′-di-*p*-tolylformamidinate, dicarboxylate = oxalate (ox) or terephthalate (tp)] featuring the *cis*-$Rh_2(form)_2$ moieties as angular components and *trans*-dicarboxylates as ligand connectors, provided evidence that no significant electronic interaction was operating among the dirhodium centres. The same electrochemical behaviour was also observed by introducing the redox active connector, *meso*-carboxyphenyl-functionalized porphyrin, 5,10-bis(4-carboxyphenyl)-15,20-diphenylporphyrin [$P(COO)_2$] into the cyclic structure. In fact, the porphyrin−dirhodium(II,II) macrocycle $[Rh_2(form)_2\{P(COO)_2\}]_2$ exhibits a CV pattern consistent with four independent redox centres releasing electrons at potential values that are mostly unchanged with respect to those of the parent species.[3]

Porphyrins are particularly attractive as building blocks for molecular materials as they couple a rich photochemistry to some interesting redox properties. They are among the most popular emitters, and indeed porphyrin-based molecules play the role of photo-active subunits in most natural photosynthetic systems,[4a] as well as in many artificial systems for solar energy conversion processes.[4b] The emission studies performed on the $[Rh_2(form)_2\{P(COO)_2\}]_2$ metallacycle revealed a luminescence decrease with respect to the free porphyrin, attributed to a reductive electron-transfer quenching of the porphyrin excited state by the dirhodium subunits.[3]

As a continuation of this study we planned the synthesis of new redox- and photo-active porphyrin−dirhodium(II,II) assemblies. The construction of such new assemblies was achieved by combining the versatile reactivity of the $[Rh_2(form)_2(O_2CCF_3)_2(H2O)_2]$ (**1**) complex[5,6] with the coordination capability of *meso*-substituted phenylporphyrins.[7]

Complex **1**, besides the well-known axial reactivity of dirhodium(II,II), allows the introduction at the equatorial position of bridging, neutral or charged, ligands.[6] Such a synthetic approach, successfully applied to the building of the above-mentioned square molecular boxes,[3] allows us to bridge carboxyphenylporphyrins at the equatorial positions of the dirhodium(II,II) species.

On the other hand, the classical axial reactivity of dirhodium(II,II) may be exploited to synthesise dirhodium(II,II)−pyridylporphyrin arrays with different shape or topology, depending on the number and geometry of the peripheral pyridyl substituents. Furthermore, dirhodium(II,II) may be used as *exo*-bidentate connectors, providing the right linear component to form square molecular boxes or grid polymers when combined with the appropriate angular component.1

In the present paper we report on the synthesis and characterization of a number of redox dirhodium(II,II)−porphyrin assemblies, with *meso*-substituted phenylporphyrins axially or equatorially ligated to dirhodium moieties. The electrochemical as well as the luminescence properties of the new multiredox systems have been also investigated.

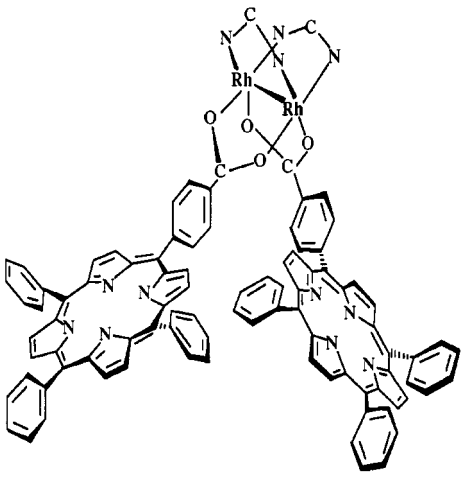

Figure 1. Structure proposed for $[Rh_2(form)_2(PCOO)_2]$ (**2**)

Results and Discussion

Synthesis and Characterization

$[Rh_2(form)_2(PCOO)_2]$ (2)

Dirhodium(II,II) systems bearing porphyrins in their equatorial positions have been synthesized by metathetical reaction of **1** with the sodium salt of *meso*-5-(4-carboxyphenyl)-10,15,20-triphenylporphyrin (PCOO). The addition of $[Rh_2(form)_2(CF_3COO)_2(H_2O)_2]$ (**1**) to a methanol/water solution of PCOONa (prepared in situ by treatment of the (carboxyphenyl)porphyrin with NaOH, see Exp. Sect.) affords $[Rh_2(form)_2(PCOO)_2]$ (**2**) in good yield. Compound **2** is a dark red-violet solid dissolving well in benzene and chlorinated solvents, sparingly in coordinating solvents such as acetone, acetonitrile, and alcohols. Elemental analysis, IR and NMR spectroscopic data are in agreement with the proposed structure (Figure 1), which retains the lantern structure of the parent complex **1**, i.e. with the two formamidinate and porphyrincarboxylate groups symmetrically bridged in a *cisoid* arrangement around the Rh_2^{4+} core.

The proton NMR spectrum of **2** does not differ significantly from those of the precursor subunits, with the exception of the pyrrole proton pattern, which consists of a rather broad singlet at $\delta = 8.88$, while in uncoordinated carboxyphenylporphyrin it appears as two doublets and one singlet. As already observed for the dirhodium−porphyrin molecular square box $[Rh_2(form)_2\{P(COO)_2\}]_2$ also bearing carboxyphenylporphyrins in the equatorial position, the electronic absorption spectrum of **2** appears as the sum of those of their constituents, suggesting that no significant electronic interaction is operating among the redox centres.

Reations of $Rh_2(form)_2(CF_3COO)_2(H_2O)_2$ (1) with Mixed meso-(4-Pyridyl)phenylporphyrins

Dirhodium(II,II)−porphyrin-based systems were also obtained by exploitation the classical axial reactivity of the

dirhodium(II,II) complexes towards Lewis bases. To this aim, the reactions of **1** with a series of functionalized *meso*-pyridylporphyrins were investigated.

$[Rh_2(form)_2(CF_3CO_2)_2(PyP)_2]$ (3)

The reaction of **1** with 5,10,15-triphenyl-20-(4-pyridyl)-porphyrin (PyP) led to the $[Rh_2(C_{15}H_{15}N_2)_2(CF_3CO_2)_2(PyP)_2]$ (**3**) adduct containing, as expected, two PyP axially coordinated to the dirhodium system via the peripheral pyridyl groups (Figure 2). The NMR spectra and the presence in the IR spectra of $\nu_{asym}(CO_2)$ and $\nu(N-C-N)$ bands at 1626 and 1594 (s) cm^{-1}, respectively, very similar to those of the parent complex **1**, confirm that the Rh_2^{4+} core remains unchanged upon the reaction.

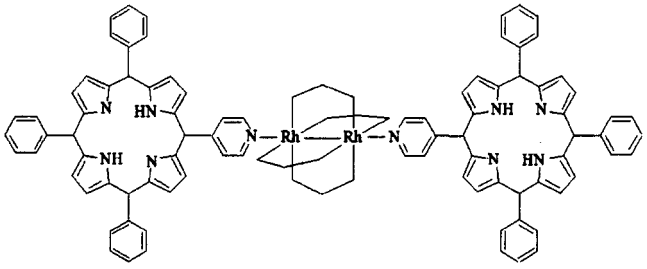

Figure 2. Structure proposed for $[Rh_2(form)_2(O_2CCF_3)_2(PyP)_2]$ (**3**)

Table 1. 300 MHz ^1H NMR chemical ($CDCl_3$, room temp.) shift for the (2,6- and 3,5-pyridyl)porphyrin protons; 2D ^1H NOESY spectra were performed to determine the correct assignment

Free porphyrins	2,6	3,5	Complexes	2,6	3,5
PyP	9.01	8.16	**3**	8.31	7.90
cis-DPyP	9.02	8.15	**4**	8.42	7.93
TPyP	9.06	8.16	**6**	7.78	7.97

Proton NMR spectroscopy is very diagnostic of the pyridylporphyrin coordination.[7] In the NMR spectra of pyridylporphyrins axially ligated to dirhodium(II,II) (present work), we found an upfield shift of the 2,6-pyridyl proton resonances (Table 1), which may be attributed to the π-back-donation from dp orbitals of the metal centre to π-anti-bonding orbitals of the porphyrin system. Consistently, the proton spectrum of **3** displays, for the 2,6-pyridyl protons, a doublet centred at δ = 8.31, with a $J_{H,H}$ coupling constant of 5.4 Hz, significantly upfield shifted as compared to free porphyrin (δ = 9.01), while the 3,5-pyridyl proton resonances are translated only by 0.26 upfield from the free one (δ = 7.90 vs. 8.16, respectively) (2D ^1H NOESY spectra were performed to determine the correct assignment). On the contrary, no shift is observed for the phenyl as well as for pyrrole proton resonances upon coordination.

$[Rh_2(form)_2(CF_3CO_2)_2(cis\text{-}DPyP)]_4$ (4)

Dirhodium(II,II) species, besides providing angular building blocks for the construction of molecular boxes, as we and others recently demonstrated,[3,8] exhibit the right properties (rigidity, geometry, and axial coordination capability) to act as *exo*-bidentate connectors of angular species leading to square molecular boxes. With this aim we explored the reactions of **1** with the 5,10-diphenyl-15,20-dipyridylporphyrin (*cis*-DPyP), which has in the past was been used successfully as an angular connector of transition metal complexes leading to square molecular boxes.[7a,7b,7f−7h]

Reaction of **1** with 1 mol-equiv. of *cis*-DPyP, in $CHCl_3$, at room temperature led to the formation of a 1:1 stoichiometry adduct, as indicated by elemental analysis and proton NMR integration data. Such a stoichiometry, in principle, may be indicative of the desired square box as well as of a polymeric species. The proper mass spectroscopic studies (MALDI, FAB- and ESI-MS), which in the lack of X-ray diffractometry data constitute the most powerful tool for establishing the nuclearity of such macrocycles, did not give unambiguous results, but, in any case showed no peaks due to long chain order oligomers.[9] No evidence of polymeric materials both as a precipitate and soluble by-products was observed, even by monitoring the reaction by NMR spectroscopy. These observations, along with the chemical and redox properties and the NMR investigations, suggest for **4** the cyclic structure showed in Figure 3.

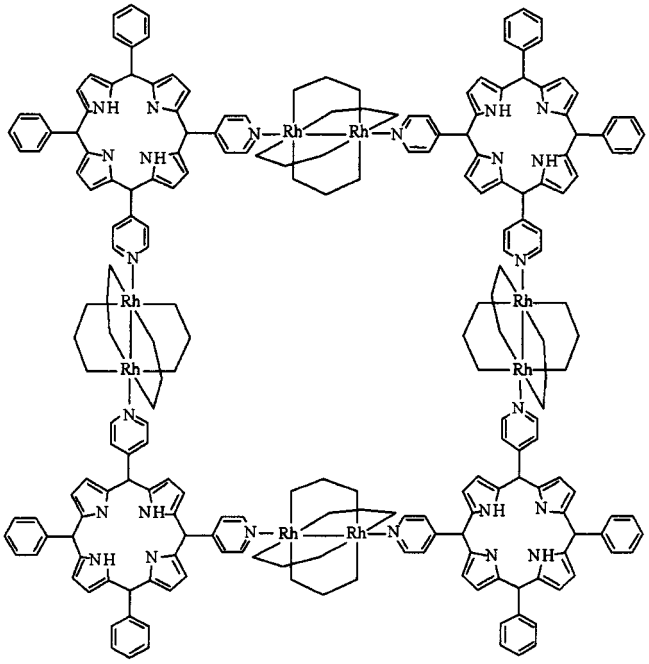

Figure 3. Structure proposed for $[Rh_2(form)_2(O_2CCF_3)_2(cis\text{-}DPyP)_2]_4$ (**4**)

This compound is, in fact, soluble in benzene and chlorinated solvents (interestingly, it is more soluble than the precursor *cis*-DPyP), but not in alcohols or acetonitrile or other coordinating solvents. Secondly, the proton spectra appear very simple and with well-resolved signals in agreement with a species at high symmetry, and finally, the redox properties are consistent with the proposed molecular structure (see below).

The inspection of the proton spectra reveals that the proton pattern resonances related to the dirhodium unit differ slightly from those of the starting building-block, while some differences are observed for the porphyrin proton resonances with respect to the free one. Consistent with the proposed structure, two equally intense doublets are observed for the (2,6- and 3,5-pyridine)porphyrin protons at $\delta = 8.42$ and 7.93, respectively, significantly shifted from free *cis*-DPyP ($\delta = 9.02$ and 8.15, respectively). Also, the phenyl as well as the pyrrole proton patterns are in agreement with a *cis* coordination for the bound *cis*-diphenyldipyridylporphyrin.[7a,7b,7f−7h] The two magnetically equivalent phenyl rings afford, in fact, two distinct proton sets for the two pairs of *ortho*- and (*meta* + *para*)-H, not shifted from free *cis*-DPyP. A slight overlapping is observed in the pyrrole proton patterns, which consist of two doublets and one singlet, accounting for four and eight protons each, respectively [three doublets are observed for free *cis*-DPyP, with a 2:4:2 proton ratio]. This is very likely caused by the pyrrole protons located inside the macrocycle that experience a downfield shift of $\delta = 0.03$ as compared to the unbound porphyrin.

$[\{Rh_2(form)_2(CF_3CO_2)_2\}_2(TPyP)]_n$ (5) and $[\{Rh_2(form)_2(CF_3CO_2)_2\}_4(TPyP)]$ (6)

The reaction of **1** with 5,10,15,20-tetrakis(4-pyridyl)porphyrin (TPyP) yielded different products depending on the molar ratio, as well as on the order of addition, of the reactants. The addition of **1** to a chloroform solution of TPyP led to a rust-coloured precipitate having a 1:2 stoichiometry between the dirhodium species and the TPyP porphyrin. Its insolubility in the most common solvents prevented its spectroscopic characterization and argues for the formation of a grid polymeric material of formula $[\{Rh_2(C_{15}H_{15}N_2)_2(CF_3CO_2)_2\}_2(TPyP)]_n$ (**5**).

When the reaction was performed in the presence of an excess of **1** (see Exp. Sect.), the species $[\{Rh_2(C_{15}H_{15}N_2)_2(CF_3CO_2)_2\}_4(TPyP)]$ (**6**), bearing four dirhodium subunits symmetrically coordinated to TpyP, was obtained in high yield. Elemental analyses and proton NMR integration agree with the requirements of the tetramer formulation as shown in Figure 4.

Consistently the aromatic region of ^1H NMR spectrum (Figure 5) shows only two doublets for the 2,6- and 3,5-pyridine protons at $\delta = 7.78$ and 7.97 ($J = 6.4$ Hz), respectively, significantly shifted with respect to those of free TPyP ($\delta = 9.06$ and 8.16, respectively), while, as expected for such a highly symmetric species, only one singlet at $\delta = 8.97$ is observed for the eight pyrrole protons, upfield shifted by 0.13 with respect to those of the free TPyP.[6d,6g] No changes are observed in the proton patterns related to the dirhodium subunits with respect to the parent complex **1**.

Complex **6** was very soluble in noncoordinating solvents (Et_2O, chlorinated solvents, etc.), remarkably more soluble than TPyP, and was stable as solid for a long time. In solution it slowly decomposed (3−4 d) releasing the parent complex **1** and an insoluble rust-coloured precipitate that was identified as **5** by IR and elemental analyses.

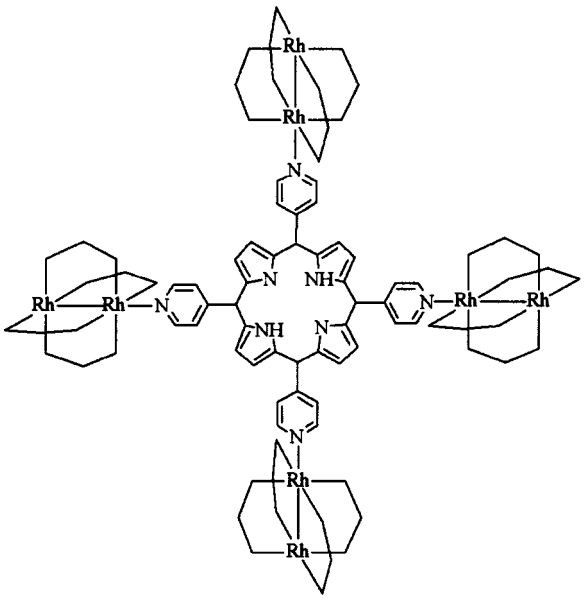

Figure 4. Structure proposed for $[\{Rh_2(form)_2(O_2CCF_3)_2\}_4(TPyP)]$ (**6**)

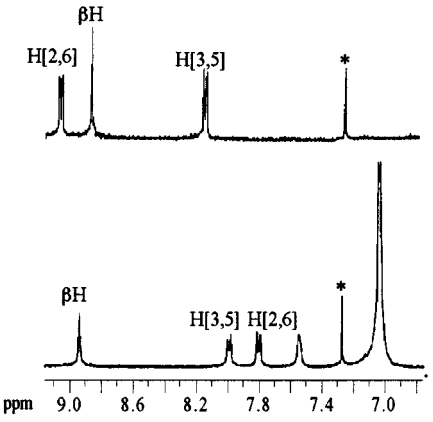

Figure 5. Aromatic region of the ^1H NMR spectra [$CDCl_3$ (*) room temp.] of TPyP (top) and (**6**) (bottom)

Electronic Spectra of 3, 4, and 6

The electronic absorption spectra of **3**, **4**, and **6** do not reveal significant modifications in the Soret and Q bands as compared to those of the unbound pyridylporphyrins, suggesting, once again, the absence of significant electronic interactions among porphyrin and the dirhodium subunits, as already observed for $[Rh_2(form)_2\{P(COO)_2\}]$ (**2**) and the square box $[Rh_2(form)_2\{P(COO)_2\}]_2$.

Electrochemistry

The new multicomponent redox systems exhibit several oxidation processes and one reduction process in the poten-

Table 2. Redox data of the new compounds; experiments were performed in argon-purged 1,2-dichloroethane solutions; all the processes are reversible except where otherwise noted; <#>: numbers of exchanged electrons

Complexes	Oxidation, *U* [V] vs. SCE[a]	Reduction, *U* [V] vs. SCE[a]
2	+0.37 <1>; +1.17 <2>[b]; +1.38 <1>[b]	−1.19 <2>[c]
3	+0.59 <1>; +1.17 <2<; 1.54[b] <1>	−1.11 <2>
4	+0.53 <4>; +1.24 <4>[c]; +1.60 <4>[b]	−1.10 <4>[c]
6	+0.60 <4>; +1.50 <4>[c]	−1.02 <1>[b]
1[d]	+0.59 <1>; +1.40 <1>	

[a] $E_{1/2}$ values are reported for reversible processes and E_{peak} values are reported for irreversible processes. [b] Irreversible process. [c] Quasi-reversible process. [d] Data obtained in dichloromethane solution.[10]

tial window examined (+ 2, −1.4 V vs. SCE), as evidenced by the redox data gathered in Table 2.

The first oxidation (+0.37 V vs. SCE) of complex **2** (Figure 6a) is attributed to the oxidation of the Rh_2^{4+} subunit, on the basis of: i) the reversibility of the process, ii) the number of electrons exchanged, iii) comparison with the potential of the oxidation process of the same subunit in the square species $[Rh_2(form)_2\{P(COO)_2\}]_2$ (+0.38 V vs. SCE).[3] Comparison with the molecular square $[Rh_2(form)_2\{P(COO)_2\}]_2$ also allowed us to attribute the second oxidation of **3** to the simultaneous one-electron oxidation of the two porphyrin subunits and the third one to the Rh_2^{5+}/Rh_2^{6+} process.

As far as compound **3** is concerned, it is interesting to note that its structure is similar to that of **2**, in particular, one "central" Rh_2^{4+} subunit is connected to two "peripheral" porphyrin fragments. However, significant differences in the properties of **2** and **3** may arise from the different nature of the linkages between subunits and from the presence, in compound **3**, of strong electron-withdrawing CF_3COO^- groups on the Rh_2^{4+} subunit (see Figures 1 and 2, respectively). Compound **3** indeed shows a redox pattern (Figure 6b) similar to that of **2**, and the attribution of the various processes to specific subunits is the same (see above). The relevant differences are the potentials of the oxidation processes centred in the Rh_2^{4+} subunit, that are substantially shifted to more positive values (ca. 200 mV; see Table 2). This is also in agreement with the oxidation reported for $[Rh_2(form)_2(CF_3COO)_2(H_2O)_2]$.[5,10]

Compound **4** exhibits three oxidation processes, each one involving four electrons. Comparison with the data of the parent compounds allows us to assign the observed processes as follows: the first process is due to four simultaneous one-electron Rh_2^{4+}/Rh_2^{5+} processes, the second one to the porphyrin subunits, and the third one to four simultaneous one-electron Rh_2^{5+}/Rh_2^{6+} processes. According to redox data shown in Table 2, the oxidation of the porphyrin fragments in **4** is more difficult than the analogous processes in **2** and **3**. This can be rationalised by considering

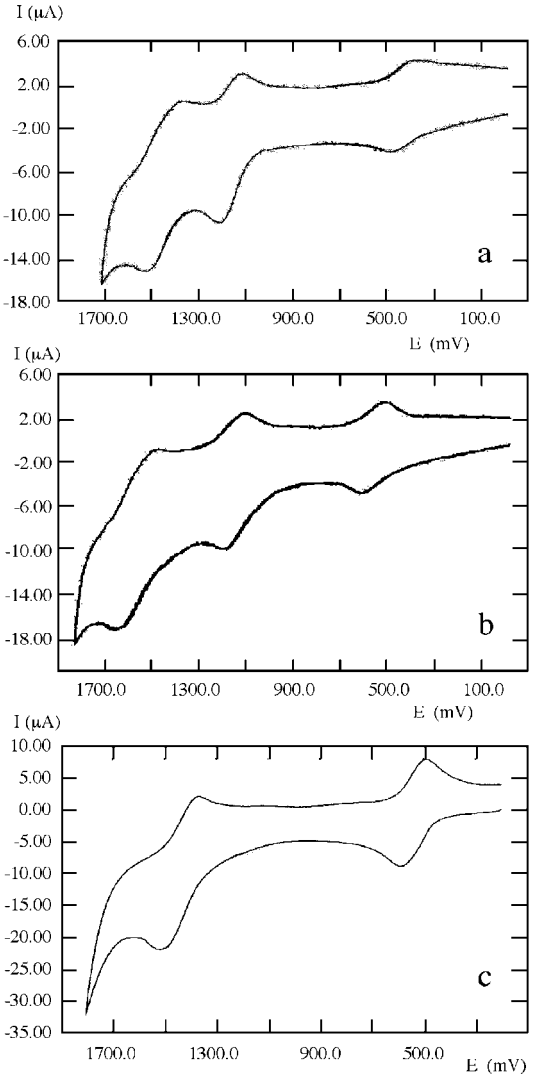

Figure 6. Cyclic voltammograms of compounds of **2** (a), **3** (b), and **6** (c); only the oxidation portion is shown

that: i) in **4** each porphyrin is connected to *two* already oxidized Rh_2^{5+} subunits when their oxidation occurs, ii) the presence of two pyridine groups most likely stabilises porphyrin orbitals.

The oxidation pattern of compound **6** is slightly different from those of the other new species reported here, in that it consists of only two processes in the potential window investigated (Figure 6c). Based on the number of exchanged electrons and of the potential values, it is possible to assign the observed processes to the successive one-electron oxidations of the four dirhodium subunits, i.e. Rh_2^{4+}/Rh_2^{5+} and Rh_2^{5+}/Rh_2^{6+} processes. The lack of the porphyrin-centred oxidation between the two dirhodium-based processes, opposed to the behaviour of the other new compounds, is probably due to the presence of the four already oxidized Rh_2^{5+} subunits, which displaces porphyrin oxidation to more positive potentials (after the second dirhodium-based oxidation). Moreover, the presence of four pyridine groups on the porphyrin fragment may also concur with this displacement.

On reduction, all the new species show a single process that is easily assigned to a porphyrin-centred reduction.[3] The number of exchanged electrons in each process is equal to the number of identical porphyrin subunits present in the examined compound. It is interesting to note that on increasing the number of pyridines the reduction process moves to less negative potentials (Table 2).

Luminescence

On the basis of the redox properties of the multicomponent systems **2**, **3**, **4**, and **6**, it was expected that the dirhodium(II,II) subunits could play the role of efficient quenchers of porphyrin-based luminescence by electron transfer. This was confirmed by the observed emission data, which are reported in Table 3 along with those related to the unbound chromophores PCOO, PyP, *cis*-DPyP, and TPyP.

Table 3. Luminescence data for the multicomponent systems **2**, **3**, **4**, and **6**, together with the related free porphyrins in air-equilibrated dichloromethane at room temperature

Compounds	Emission maxima [nm][a]	τ [ns]	ΔG [eV][b]
P(COO)	648	8.6	
2	648	1.5	−0.35
PyP	650	8.5	
3	no emission	−	−0.21
cis-DPyP	655	8.5	
4	no emission	−	−0.20
TPyP	655	8.5	
6	no emission	−	−0.27

[a] Only the highest-energy feature of the emission spectrum, taken as the E_{00} energy, is reported. [b] Driving force for the reductive electron transfer quenching, calculated as in Equation (1) (see text).

As expected, the uncoordinated porphyrins are strong emitters under the experimental conditions used. However, such an emission is significantly reduced in **2**, whereas **3**, **4**, and **6** do not exhibit any emission at all. This finding clearly indicates that a quenching of the porphyrin-based emission occurs in the studied multicomponent complexes due to the presence of the dirhodium subunits. A possible mechanism for the quenching is reductive electron transfer. Actually, the driving force ΔG for reductive electron transfer quenching of the porphyrin-based excited state by the dirhodium(II,II) subunits can be approximated by Equations (1) and (2), where entropy contributions and work terms are neglected.[11]

$$\Delta G = e[E_{ox} - {}^*E_{red}] \quad (1)$$

$${}^*E_{red} = E_{red} + E_{00} \quad (2)$$

In these Equations, E_{ox} is the oxidation potential of the dirhodium(II,II) subunit(s), E_{red} is the reduction potential of the porphyrin subunit(s), and E_{00} is the energy of the luminescent excited state of the corresponding model compounds, approximate to the highest-energy feature of the emission spectra. The ΔG values obtained are also shown in Table 2 and indicate that electron transfer from the dirhodium subunits to the excited porphyrin chromophores is moderately exergonic in all the cases. Electron transfer rate constants for moderately exergonic processes depend on the electronic interactions between the partners, in turn governed by several factors such as donor−acceptor distance, nature of spacers, and reorganization energy.[11] Compound **2** is luminescent, although with a reduced lifetime compared to PCOO. So the rate of the process k_{et} for this system can be easily obtained by Equation (3), in which τ_0 is the luminescence lifetime of the free porphyrin, PCOO, and τ is the luminescence lifetime of the species in the presence of the quencher, **2**.

$$k_{et} = 1/\tau - 1/\tau_0 \quad (1)$$

From the data in Table 3, k_{et} is 5.2×10^8 s^{-1} in **2**. It could be noted that this value is smaller than that estimated by a different method (luminescence quantum yield comparison between the free chromophore and chromophore-quencher systems) for a molecular square basically containing the same components.[3] However, in complex **2** each chromophore is connected to a single dirhodium(II,II) quencher, while in the molecular square compound reported in literature the chromophore was connected to two potentially quencher subunits, which both could contribute to the quenching process.

Complexes **3**, **4**, and **6** do not exhibit any emission, so the electron transfer rate constants cannot be evaluated by Equation (3). However, the complete quenching of the porphyrin emission in these complexes suggests that the electron transfer rate constants in **3**, **4**, and **6** are probably at least one order of magnitude larger than the value obtained for **3**. Differences in the driving force cannot be responsible for the difference in the electron-transfer rate, in that they are in the opposite direction (Table 3). The reason probably lies in the nature of the linkage between the chromophore(s) and the quencher subunits. Apparently, the pyridine linkage which is present in **3**, **4**, and **6** allows a better electronic coupling between donor and acceptor partners than the bridged carboxylate one, operating in **2** and in the molecular square $[Rh_2(form)_2\{P(COO)_2\}]_2$.

It should be noted that the occurrence of electron transfer between porphyrin and dirhodium subunits, which indicates that electronic coupling between the subunits takes place, is not in contradiction with the negligible interactions inferred by absorption spectra and redox properties. It is well known that electronic coupling as small as tens of cm^{-1}, which hardly cause changes in absorption spectra and redox properties of the individual subunits of the multicomponent arrays, are sufficient to promote fast intercomponent energy and/or electron-transfer processes.[12]

Conclusions

In the present paper, we have reported the results of our studies aimed at the synthesis and characterization of dirhodium−porphyrin assemblies as models of photoactive multiredox systems. The synthesis of such new assemblies

was achieved by combining the versatile reactivity, both axial and equatorial, of the $[Rh_2(form)_2(O_2CCF_3)_4(H_2O)_2]$ (**1**) complex with the coordination capability of *meso*-substituted phenylporphyrins. In this way, systems, featuring pyridylporphyrins axially coordinated or (carboxyphenyl)porphyrins equatorially bridged to the dirhodium subunits, were readily obtained. We have also explored the possibility of building dirhodium−porphyrin-based molecular square boxes. The capability of **1** to act as a precursor for new mixed dirhodium complexes, via the *cis*-$Rh_2(form)_2$ moieties, has already been exploited to synthesize the molecular square box $[Rh_2(form)_2\{P(COO)_2\}]_2$.[3] The square molecular box $[Rh_2(form)_2(CF_3CO_2)_2(cis\text{-DPyP})]_4$ (**4**), in which the dirhodium subunit acts as an *exo*-bidentate ligand, was obtained by assembling **1** with the *cis*-5,10-diphenyl-15,20-dipyridylporphyrin (*cis*-DPyP), which in turn constitutes the angular building block. It should also be remarked that the synthesis of the tetramer species $[\{Rh_2(form)_2(CF_3CO_2)_2\}_4(TPyP)]$ was achieved by reaction of **1** with 5,10,15,20-tetrakis(4-pyridyl)porphyrin (TPyP).

All the new systems undergo many redox processes in the potential window under investigation. It is important to stress that the redox patterns, especially in the oxidation part, are strictly related to the structure of the compounds.

In the multicomponent porphyrin−dirhodium assemblies studied here, the porphyrin-based emission is significantly quenched, most likely by reductive electron transfer from the dirhodium subunits to the excited porphyrin chromophores, a process which is moderately exergonic in all the cases. The rate constants of the processes appear to be larger in the compounds in which a pyridine linkage between dirhodium and porphyrin subunits is present compared with the compound in which the linkage is realized through bridging carboxylates, suggesting that the donor−acceptor electronic coupling is larger in the former cases.

Experimental Section

Materials: The starting complex $[Rh_2(form)_2(CF_3COO)_2(H_2O)_2]$ was prepared according to literature data.[5] The *meso*-5-(4-carboxyphenyl)-10,15,20-triphenylporphyrin was purchased from Mid-Century Company, Illinois. All other chemicals are commercially available and used as supplied. None of the compounds here reported were air-sensitive, but all reactions were carried out under dry nitrogen. Elemental analyses were performed by REDOX snc Laboratorio di Microanalisi, Monza, Italy.

Apparatus: Infrared spectra were recorded on KBr pellets with a Perkin−Elmer FT 1720X spectrometer. Electronic absorption spectra were recorded with a Perkin−Elmer Lambda 5 UV/Visible spectrophotometer. The NMR measurements were performed with a Bruker AMX 300 spectrometer using standard pulse sequences. Electrochemical measurements were carried out in argon-purged 1,2-dichloroethane at room temperature with a PAR 273 multipurpose equipment interfaced to a PC. The working electrode was a glassy carbon (8 mm^2, Amel) electrode. The counter electrode was a Pt wire, and the quasi-reference electrode was an Ag wire (ferrocene was used as internal standard). The concentration of the complexes was about 5×10^{-4} M. Tetrabutylammonium hexafluorophosphate was used as supporting electrolyte and its concentration was 0.05 M. Cyclic voltammograms were obtained at scan rates of 20, 50, 200, and 500 mV/s. For reversible processes, half-wave potentials (vs. SCE) were calculated as the average of the cathodic and anodic peaks. The criteria for reversibility were the separation between cathodic and anodic peaks, the close to unity ratio of the intensities of the cathodic and anodic currents, and the constancy of the peak potential on changing the scan rate. For irreversible processes, the values reported in Table 2 are the peaks estimated by differential pulse voltammetry (DPV). The number of exchanged electrons was measured with differential-pulse voltammetry (DPV) experiments performed with a scan rate of 20 mV/s, a pulse height of 75 mV, and a duration of 40 ms. Experimental error on the redox potentials was ± 10 mV. For the irreversible or quasi-reversible processes, an estimation of the number of the electrons involved can be inferred by current intensity of the anodic (for oxidation processes) or cathodic (for reduction processes) peaks. The luminescence experiments were performed in air-equilibrated dichloromethane solution at 298 K. Luminescence spectra were obtained with a Jobin Yvon-Spex Fluoromax 2 fluorimeter (experimental error on luminescence maxima was ± 4 nm). The spectra were corrected for detector response. The luminescence lifetimes were measured by an Edinburgh FL 900 Single-Photon-Counting Spectrometer (experimental error on lifetimes was ± 10%).

Preparations

$Rh_2(form)_2(PCOO)_2$ (2): To a mixture of methanol (50 mL) and 5-(4-carboxyphenyl)-10,15,20-triphenylporphyrin (0.150 g, 0.228 mmol) was added an aqueous solution (5 mL) of NaOH (0.010 g, 0.250 mmol). The resulting solution was stirred for ca. 1 h and then filtered. A chloroform solution (10 mL) of **1** (0.139 g, 0.152 mmol) was added dropwise to the filtrate, and the resulting mixture stirred for 36 h. After this time, the resulting brown red solid was collected by filtration, dissolved in 30 mL of benzene and the resulting mixture filtered. By addition of *n*-heptane (30 mL) to the filtrate, **2** was obtained as a red-brown microcrystalline precipitate. Yield: 0.185 g (62%). $C_{120}H_{88}N_{12}O_4Rh_2$ (1967.92): calcd. C 73.24, H 4.51, N 8.54; found C 73.34, H 4.58, N 8.60. IR (KBr pellet, nujol mulls): $\tilde{\nu}$ = 1619 [m, $\nu_{asym}(CO_2)$], 1593 cm^{-1} [s, ν(N−C−N)]. UV/Vis (C_6H_6): λ_{max} = 423.8, 514.4, 549.0, 591.2, 649.2 nm. ^{1}H NMR (CD_2Cl_2): δ = −2.66 (s, 4 H), 2.32 (s, 12 H), 7.16 (m, 16 H), 7.75 (m, 22 H), 8.20 (m, 14 H), 8.50 (d, 4 H, J = 8 Hz), 8.83 (br. s, 16 H).

$[Rh_2(form)_2(CF_3CO_2)_2(PyP)_2]$ (3): A chloroform solution (20 mL) of **1** (0.100 g, 0.110 mmol) was added to a solution of PyP (0.135 g, 0.220 mmol) in the same solvent (50 mL), and the resulting red-violet solution stirred for ca. 24 h. After this time, the solution was filtered and the solvents were evaporated to dryness using a rotary evaporator. The residue was washed with *n*-hexane and recrystallized from chloroform/*n*-heptane. Compound **3** was obtained as a dark-violet precipitate. Yield: 0.208 g (90%). $C_{120}H_{88}F_6N_{14}O_4Rh_2$ (2109.93): calcd. C 68.31, H 4.20, F 5.40, N 9.29; found C 68.12, H 4.30, F 5.35, N 9.22. IR (KBr pellet, nujol mulls): $\tilde{\nu}$ = 1626 [m, $\nu_{asym}(CO_2)$], 1594 cm^{-1}[s, ν(N−C−N)]. UV/Vis ($CHCl_3$): λ_{max} = 419, 515, 549, 589, 644 nm. ^{1}H NMR ($CDCl_3$): δ = −2.79 (s, 2 H), 2.22 (s, 12 H), 7.02 (m, 16 H), 7.54 (t, br, 2 H), 7.77 (m, 20 H), 7.90 (d, J = 5.4 Hz, 4 H), 8.24 (m, 10 H), 8.31 (d, J = 5.4 Hz, 4 H), 8.82 (d, 4 H, J = 4.83 Hz), 8.86 (s, 8 H), 8.95 (d, 4 H, J = 4.83 Hz).

$[Rh_2(form)_2(CF_3CO_2)_2(cis\text{-DPyP})]_4$ (4): A chloroform solution (75 mL) of *cis* -DPyP (0.087 g, 0.142 mmol) was added to a solution of **1** (0.130 g, 0.142 mmol) in the same solvent (30 mL). The resulting red-violet solution was stirred for 24 h, then filtered and

dried using a rotary evaporator. The residue was washed with *n*-hexane, and then dissolved in benzene (50 mL) and the resulting solution filtered. The addition of *n*-heptane to the filtrate afforded **5** as a dark-violet solid. Yield: 0.138 g (65%). $C_{76}H_{58}F_6N_{10}O_4Rh_2$ (5980.70): calcd. C 61.05, H 3.91, F 7.62, N 9.37; found C 60.95, H 3.96, F 7.49, N 9.29. IR (KBr pellet, nujol mulls): $\tilde{\nu}$ = 1622 [m, $\nu_{asym}(CO_2)$], 1592 cm^{-1} [s, ν(N−C−N)]. UV/Vis ($CHCl_3$): λ_{max} = 419, 515, 549, 589, 644 nm. ^1H NMR ($CDCl_3$): δ = −2.76 (s, 2 H), 2.13 (s, 12 H), 7.00 (m, 16 H), 7.51 (t, br, 2 H), 7.77 (m, 6 H, *m*-,*p*-H Ph), 7.93 (d, br, 4 H), 8.2 (m, 4 H, *o*-H Ph), 8.42 (d, br, 4 H), 8.78 (d, 2 H, J = 4.62 Hz), 8.87 (s, 4 H), 8.93 (d, 2 H, J = 4.62 Hz).

$[\{Rh_2(form)_2(CF_3CO_2)_2\}_2(TPyP)]_n$ (5): A chloroform solution (70 mL) of TPyP (0.040 g, 0.066 mmol) was added to a solution of **1** (0.120 g, 0.132 mmol) in the same solvent (30 mL). Immediately, **6** was formed as a red-brown precipitate. The resulting mixture was stirred overnight, and then the precipitate was collected by filtration, washed several times with $CHCl_3$, and dried in vacuo. Yield: 0.141 g (90%). $C_{108}H_{86}F_{12}N_{16}O_8Rh_4$ (2375.59): calcd. C 54.61, H 3.65, F 9.60, N 9.43; found C 54.43, H 3.64, F 9.43, N 9.44. IR (KBr pellet, nujol mulls): $\tilde{\nu}$ = 1626 [m, $\nu_{asym}(CO_2)$], 1594 cm^{-1} [s, ν(N−C−N)]. The low solubility of **5** prevented a full spectroscopic characterization.

$[\{Rh_2(form)_2(CF_3CO_2)_2\}_4(TPyP)]$ (6): A chloroform solution (70 mL) of TpyP (0.033 g,053 mmol) was added to a solution of **1** (0.120 g, 0.218 mmol) in the same solvent (30 mL). The resulting solution was stirred for 24 h and then left to stand for ca. 2 d. Then the solution was dried using a rotary evaporator, and the residue washed with *n*-hexane. Crystallization of the residue by diethyl ether/*n*-hexane (0 °C) afforded **6** as a dark-red microcrystalline solid. Yield: 0.135 g (60%). $C_{176}H_{146}F_{24}N_{24}O_{16}Rh_8$ (4132.48): calcd. C 51.15, H 3.56, F 11.03, N 8.13; found C 51.30, H 3.62, F 11.00, N 8.21. IR (KBr pellet, nujol mulls): $\tilde{\nu}$ = 1626 [m, $\nu_{asym}(CO_2)$], 1594 cm^{-1} [s, ν(N−C−N)]. UV/Vis ($CHCl_3$): λ_{max} = 419, 515, 549, 589, 644 nm. ^1H NMR ($CDCl_3$): δ = −2.90 (s, 2 H), 2.26 (s, 48 H), 7.0 (m, 64 H), 7.52 (t, br, 8 H), 7.78 (d, J = 6.4 Hz, 8 H), 7.97 (d, J = 6.4 Hz, 8 H), 8.97 (s, 8 H).

Acknowledgments

We thank the Italian CNR and the MURST for financial support.

[1] [1a] M. R. Wasielewski, *Chem. Rev.* **1992**, 435−461. [1b] H. Kurreck, M. Huber, *Angew. Chem. Int. Ed. Engl.* **1995**, *34*, 849−866. [1c] J.-M. Lehn, *Supramolecular Chemistry*, VCH Publishers, New York, **1995**. [1d] P. L. Boulas, M. Gòmez-Kaifer, L. Echegoyen, *Angew. Chem. Int. Ed.* **1998**, *37*, 216−247.

[2] [2a] S. Leninger, B. Olenyuk, P. J. Stang, *Chem. Soc. Rev.* **2000**, 853−908. [2b] B. Olenyuk, A. Fechtenkotter, P. J. Stang, *J. Chem. Soc., Dalton Trans.* **1998**, 1707−1729. [2c] M. Fujita, *Chem. Soc. Rev.* **1998**, 417−425. [2d] B. J. Hollyday, C. A. Mirkin, *Angew. Chem. Int. Ed.* **2001**, *40*, 2022−2043. [2e] P. N. W. Baxter, R. G. Khoury, J.-M. Lehn, G. Baum, D. Fenske, *Chem. Eur. J.* **2000**, 4140−4148 and refs. therein.

[3] S. Lo Schiavo, G. Pocsfalvi, S. Serroni, P. Cardiano, P. Piraino, *Eur. J. Inorg. Chem.* **2000**, 1371−1375.

[4] [4a] J. Deinsenhofer, H. Michel, *Angew. Chem. Int. Ed. Engl.* **1989**, *28*, 829−847. [4b] D. Gust, T. A. Moore, A. L. Moore, *Acc. Chem. Res.* **2001**, *34*, 40−48, and refs. therein. [4c] S. Anderson, H. Anderson, A. Bashall, M. McPartlin, J. K. M. Sanders, *Angew. Chem. Int. Ed. Engl.* **1995**, *34*, 1096−1099. [4d] A. Harriman, J. Sauvage, *Chem. Soc. Rev.* **1996**, 41−48. [4e] R. V. Slone, D. I. Yoon, R. M. Calhoun, J. T. Hupp, *J. Am. Chem. Soc.* **1995**, *117*, 11813−11814. [4f] A. Prodi, M. T. Indelli, C. J. Kleverlaan, F. Scandola, E. Alessio, T. Gianferrara, L. G. Marzilli, *Chem. Eur. J.* **1999**, 2668−2679. [4g] K. Sugiura, Y. Fujimoto, Y. Sakata, *Chem. Commun.* **2000**, 1105−1106.

[5] P. Piraino, G. Bruno, S. Lo Schiavo, F. Laschi, P. Zanello, *Inorg. Chem.* **1987**, *26*, 91−96.

[6] [6a] P. Piraino, G. Bruno, S. Lo Schiavo, F. Laschi, P. Zanello, *Inorg. Chem.* **1987**, *26*, 2205−2211. [6b] G. A. Rizzi, M. Casarin, E. Tondello, P. Piraino, G. Granozzi, *Inorg. Chem.* **1987**, *26*, 3406−3409. [6c] E. Rotondo, B. E. Mann, P. Piraino, G. Tresoldi, *Inorg. Chem.* **1989**, *28*, 3070−3073. [6d] E. Rotondo, G. Bruno, F. Nicolò, S. Lo Schiavo, P. Piraino, *Inorg. Chem.* **1991**, *30*, 1195−1200. [6e] P. Piraino, G. Tresoldi, S. Lo Schiavo, *Inorg. Chim. Acta* **1993**, *203*, 101−105. [6f] G. Bruno, G. De Munno, G. Tresoldi, S. Lo Schiavo, P. Piraino, *Inorg. Chem.* **1992**, *31*, 1538−1540. [6g] S. Lo Schiavo, M. S. Sinicropi, G. Tresoldi, C. G. Arena, P. Piraino, *J. Chem. Soc., Dalton Trans.* **1994**, 1517−1522. [6h] G. Tresoldi, G. De Munno, F. Nicolò, S. Lo Schiavo, P. Piraino, *Inorg. Chem.* **1996**, *35*, 1377−1381.

[7] [7a] C. M. Drain, J.-M. Lehn, *Chem. Commun.* **1994**, 2313−2315. [7b] J. Fan, J. A. Whiteford, B. Olenyuk, M. D. Levin, P. J. Stang, E. B. Fleisher, *J. Am. Chem. Soc.* **1999**, *121*, 2741−2752. [7c] P. J. Stang, J. Fan, B. Olenyuk, *Chem. Commun.* **1997**, 1453−1454. [7d] R. V. Slone, J. T. Hupp, *Inorg. Chem.* **1997**, *36*, 5422−5423. [7e] L. Pan, B. C. Noll, X. Wang, *Chem. Commun.* **1999**, 157−158. [7f] E. Iengo, B. Milani, E. Zangrando, S. Geremia, E. Alessio, *Angew. Chem. Int. Ed.* **2000**, *39*, 1096−1099. [7g] E. Alessio, M. Macchi, S. Heath, L. G. Marzilli, *Chem. Commun.* **1996**, 1411−1412. [7h] E. Alessio, E. Ciani, E. Iengo, V. Y. Kukushkin, L. G. Marzilli, *Inorg. Chem.* **2000**, *39*, 1434−1443. [7i] E. Alessio, S. Geremia, S. Mestroni, E. Iengo, B. Milani, E. Zangrando, *Inorg. Chem.* **1999**, *38*, 869−875 and refs. therein.

[8] [8a] F. A. Cotton, L. M. Daniels, C. Lin, C. A. Murrillo, *J. Am. Chem. Soc.* **1999**, *121*, 4538−4539. [8b] R.-P. Bonar-Law, T. D. McGrath, N. Singh, J. F. Bickley, A. Steiner, *Chem. Commun.* **1999**, 2457−2458.

[9] It is very likely that thermal and collision dissociation of the assembly occurs under the applied ESI conditions, as no pyridylporphyrin−dirhodium aggregate studied here gave significant ES mass spectra.

[10] S. Lo Schiavo, G. Bruno, P. Zanello, F. Laschi, P. Piraino, *Inorg. Chem.* **1997**, *36*, 1004−1012.

[11] *Electron Transfer in Chemistry*, vols. 1−5 (Ed.: V. Balzani), Wiley-VCH, Weinheim, **2001**.

[12] [12a] F. Scandola, M. T. Indelli, C. Chiorboli, C. A. Bignozzi, *Top Curr. Chem.* **1990**, *158*, 73−95. [12b] V. Balzani, A. Juris, M. Venturi, S. Campagna, S. Serroni, *Chem. Rev.* **1996**, *96*, 759−778.

Received June 27, 2001
[I01236]